Magnetic vortices in tridimensional nanomagnetic caps observed using transmission electron microscopy and magnetic force microscopy

Márcio M. Soares,[1,2] Emilio de Biasi,[1,2] Letícia N. Coelho,[1,3] Maurício C. dos Santos,[4] Fortunato S. de Menezes,[5] Marcelo Knobel,[2] Luiz C. Sampaio,[6,*] and Flávio Garcia[1]

[1]*Laboratório Nacional de Luz Síncroton, Giuseppe Máximo Scolfaro, 10000, Campinas, São Paulo 13.084-971, Brazil*

[2]*Instituto de Física "Gleb Wataghin," Universidade Estadual de Campinas, Campinas, São Paulo 13.083-970, Brazil*

[3]*Departamento de Física, Universidade Federal de Minas Gerais, Avenida Antônio Carlos, 6627, Belo Horizonte, Minas Gerais 31270-901, Brazil*

[4]*Departamento de Física, Universidade Federal Rural do Rio de Janeiro, BR 465 Km 7, Seropédica, Rio de Janeiro 23890-000, Brazil*

[5]*Universidade Federal de Lavras, Departamento Ciências Exatas (DEX), Lavras, Minas Gerais 37.200-000, Brazil*

[6]*Centro Brasileiro de Pesquisas Físicas, Xavier Sigaud, 150, Rio de Janeiro, Rio de Janeiro 22.290-180, Brazil*

(Received 8 January 2008; revised manuscript received 29 April 2008; published 2 June 2008)

Magnetic domain formation on three-dimensional nanostructures was investigated. Co/Pd multilayers were deposited on polystyrene nanospheres (50–1000 nm) to form a magnetic cap with variable thickness. High resolution transmission electron microscopy and magnetic force microscopy images, allied with micromagnetic simulations, were used to correlate the three-dimensional shape of the caps with their domain structures. For smaller spheres (50–100 nm), the caps are segmented into nanopillars ($\simeq$10 nm) oriented toward the radial direction. For larger spheres (500–1000 nm), the cap is a continuous film with the magnetization forming a vortex at the top of the cap, with a core well larger than the ones observed in planar disks.

DOI: 10.1103/PhysRevB.77.224405 PACS number(s): 75.75.+a, 75.60.Ch, 75.70.−i

I. INTRODUCTION

One of the most interesting aspects of nanostructured magnetic materials is the possibility of tailoring the magnetic properties, changing its size and shape. Such small structures can assume different magnetic domain configurations and, therefore, different magnetic and electronic transport properties.[1,2]

Nanostructures based in Co/Pd and Co/Pt multilayers have been intensively studied in the last years.[3–9] An interesting feature of Co/Pd(Pt) thin films, which can be even improved in artificial nanostructures, is the possibility of modifying the magnetic anisotropy (from perpendicular to in plane, for instance), simply by varying the parameters such as the number of repeats, buffer layer thickness, relative Co/Pd(Pt) thicknesses,[3–8] or by ion irradiation.[9] A further parameter that can also be modified is the substrate curvature. Magnetic films deposited onto small spheres, such as polystyrene nanospheres, form a cap with a variable thickness that is actually a nice and simple bottom-up process to obtain a nanosized system.

Among the magnetic structures that can be formed in small scales, the magnetization vortex has received a large interest in the last years. Since its first experimental observation in small permalloy disks,[10] an increasing activity on the study of magnetic vortex properties has been recently reported. Diverse aspects such as the vortex core structure,[11,12] chirality,[13] and magnetization reversal dynamics induced by a pulsed field[14] or by a polarized spin current[15–17] have been explored, just to cite a few studies. Aside from this effort, the influence of the nanostructure shape on the vortex properties still remains unexplored. In spite of many magnetic nanostructures that have been experimentally and theoretically studied so far, a deeper understanding of the relationship between the domain pattern, shape, and atomic microstructure is still lacking mainly in three-dimensional structures.

Using a combination of high resolution microscopies and magnetic measurement techniques, allied with micromagnetic simulations, we report, herein, the magnetic domain structures in small caps grown on nanospheres. For large spheres (diameter 500 and 1000 nm), the magnetic vortex structure was observed with a core whose size can be 30 times larger than the ones observed in planar disks.[10] On the other hand, for small spheres (50 and 100 nm), the film is no longer continuous; it is segmented into nanopillars ($\sim$10 nm) oriented toward the radial direction. The present work reports an experimental observation of the magnetization vortices on three-dimensional nanostructures and aims to show how the magnetic configuration in small scales can be affected by the shape and atomic microstructure.

II. EXPERIMENT

A. Sample preparation

To obtain small caps, we have deposited a magnetic thin film onto the nanospheres of polystyrene monodisperse with diameters of 50, 100, 500, and 1000 nm. The spheres self-organize in a hexagonal closed-packed array, forming one or several layers. In this work, we report the data for the samples with a single layer of spheres. Initially, the substrate surface has to be treated to become hydrophilic in order to spread the spheres over the entire substrate (7×7 mm^2). The Si substrate is cleaned and exposed to O_2 plasma for 30 min (100 W and 600 mTorr). Isopropanol alcohol (20 μL) is then dropped over the substrate and then a few microliters (e.g., 1.25 μL for spheres with size of 1000 nm) of nanospheres suspended in water (2.5 % wt) are added. Such quantities were calculated in order to cover the entire substrate with one monolayer. During alcohol evaporation, the convec-

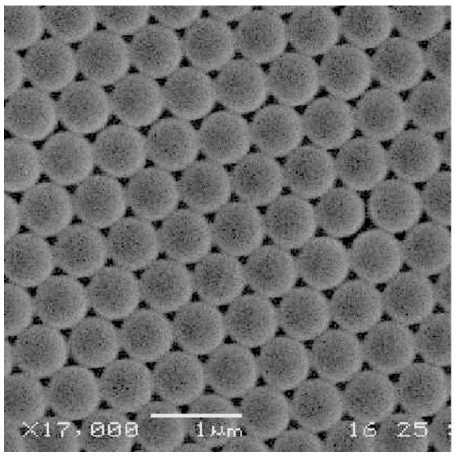

FIG. 1. SEM image of an ensemble of spheres with a diameter of 500 nm.

tion motion homogeneously spreads the spheres and a thin water layer with a thickness comparable to the sphere diameter remains at the end. The water evaporates and the superficial tension pulls the spheres out toward the water film border, providing the bi-dimensional growth of the sphere array (see also Ref. 18). Usually, the spheres cover most part of the substrate surface with one monolayer. The organization of the spheres was verified by a scanning electron microscopy (SEM) and atomic force microscopy (AFM). Figure 1 shows a typical image for an array of spheres.

After the sphere array preparation, the Pd(10)/[Co(X)/Pd(1 nm)]×6 multilayers (X=0.8, 0.6, 0.4, and 0.2 nm) were grown by dc sputtering onto the planar Si/SiO_2 substrates and nanospheres. All depositions were performed during the same sputtering run in order to ensure the same growth conditions. The substrates were kept rotating in order to avoid shadow effects, leading to a homogeneous deposition. Due to the sphere topography, the deposited film assumes a variable thickness along the surface, being thicker at the top and very thin close to the sphere equator.

In planar films, depending on the Co thickness, the magnetic anisotropy favors the out-of-plane or in-plane magnetization due to the competition between the surface and the shape anisotropies, respectively. For thicker films, the surface anisotropy, which is proportional to the inverse of the film thickness, decreases and the shape anisotropy prevails (see, for instance, Ref. 19). Recently, interesting results on Co/Pd multilayers with out-of-plane magnetic anisotropy deposited onto the polystyrene nanospheres were reported.[20,21] The caps are single domains and are magnetized up or down in relation to the plane defined by the spheres. We have focused our work on the Co/Pd multilayers with 0.8 nm Co film where the magnetization is in plane. Deposited on the caps, this Co thickness corresponds to an interesting magnetic domain structure leading to the formation of vortices. We have also studied the caps with 0.4 nm Co film and found results equivalent to those found in Refs. 20 and 21.

B. Film structure by transmission electron microscopy

The film thickness and its inner structure were obtained by TEM (JEOL HRTEM-JEM 3010 URP) in cross-section

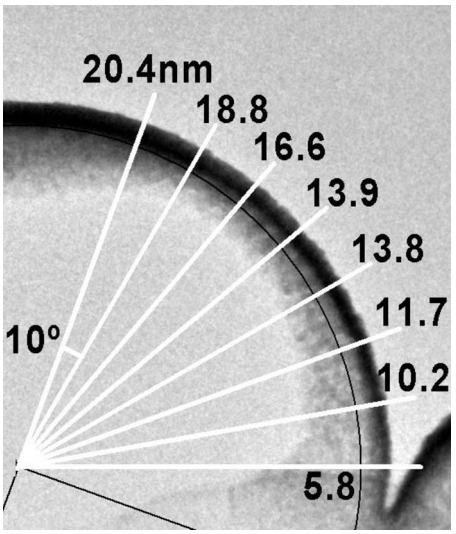

FIG. 2. TEM cross-section image of a single sphere with a diameter of 500 nm. The cap thickness is shown for each 10°

mode. The sample preparation was performed by ion milling at low temperature in order to avoid heating the latex spheres. The milling intensity was optimized to avoid dislocations in the film structure.

Figure 2 shows a TEM image for a sphere 500 nm large. This image is a representative for the large spheres (both 500 and 1000 nm). Since the sphere was sliced approximately at the center, the film thickness at the top of the cap is approximately at the multilayer nominal deposition, which is 20.4 nm, and it continuously varies following a cosine angular dependence (see Fig. 3). Since the sputtering guns are located far enough from the substrates, such cosine dependence is expected although it has never been reported before. The films exhibit a polycrystalline fcc structure with some texture, which is commonly observed in sputtered multilayers deposited on planar substrates.[22] Independent of the sphere curvature, such texture was also observed for the caps and the grains have a mean size of approximately 6 nm (see Fig. 4). The vertical lines show the limit between the grains; the atomic ordering is more visible in a high resolution image. Notice that although the sphere acts as a curved substrate, the film remains continuous at least for 500 and 1000 nm. Furthermore, also due to the sphere curved topography, the film close to the sphere equator becomes inhomogeneous,

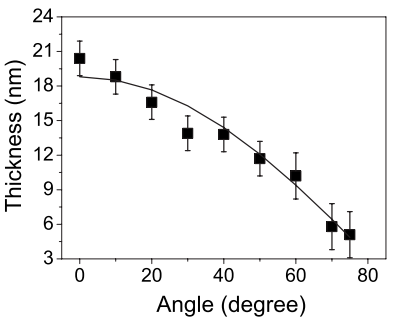

FIG. 3. Film thickness for different points on the cap shown on Fig. 2. The line is a guide for the eyes.

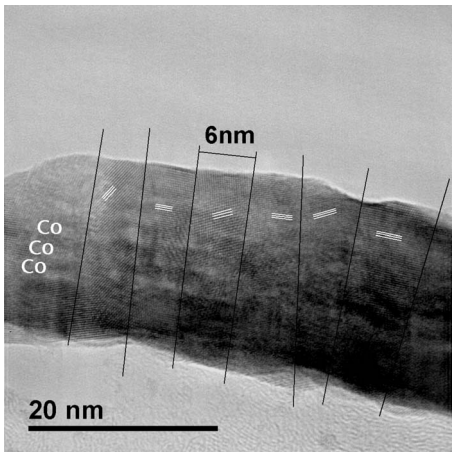

FIG. 4. Detail of the top of the cap taken from Fig. 2. The white horizontal lines are stacking of the Co/Pd multilayers.

especially the multilayer structure and the interface definition. It happens because, at the edge, the film deposition is almost grazing to the sphere surface. As can be seen in Fig. 5, from the image of the edge, some granular structure arises and the Co/Pd interfaces are no longer flat, producing a variation on the magnetic anisotropy[9] (we will return to this point later).

Figures 6 and 7 show TEM images for spheres with diameters of 50 and 100 nm. They are the representative for the small size spheres. For these spheres, the film thickness is comparable to the sphere diameter. Furthermore, the curvature produces a tension on the film, which is large enough to cause the segmentation of the cap into nanopillars. The nanopillars are radially oriented with lateral dimensions of about 7 and 11 nm at the base and the top, respectively.

From the TEM analysis, it becomes clear that the use of nanospheres as substrates is interesting to produce nanostructures such as caps with the possibility to alter the inner structure, changing the relative dimensions between the film thickness and the sphere size.

C. Magnetic structure by magnetic force microscopy

The atomic/magnetic force images were obtained with a multimode III microscope (Veeco Instruments) using a

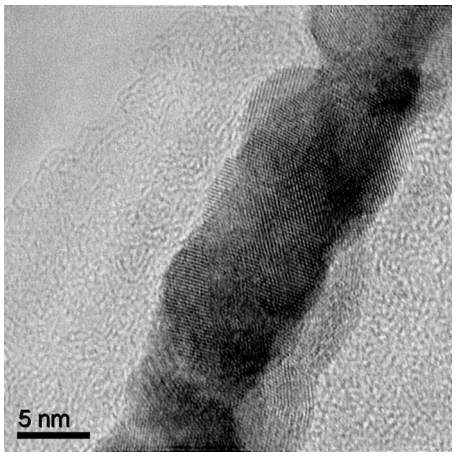

FIG. 5. Detail of the edge of the cap taken from Fig. 2.

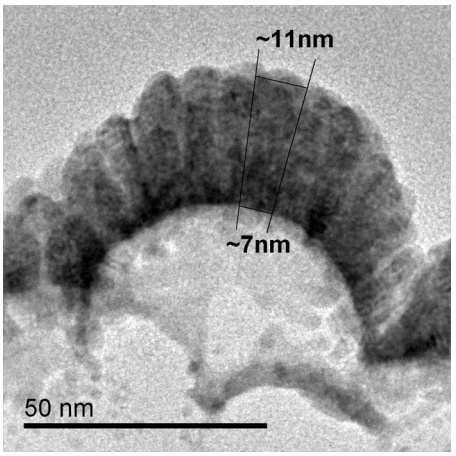

FIG. 6. TEM cross-section image of a single sphere with a diameter of 50 nm.

Co-Cr covered Si probe (typical curvature radius of 30 nm) in tapping mode. The magnetic measurements were performed at a distance between the sample and the probe from 30 to 100 nm (lift mode), where no van der Waals forces are expected to be detected. Therefore, the magnetic image is purely due to the interaction between the magnetized probe and the sample stray magnetic field. The tests with nonmagnetic tips with the same experimental conditions yielded no magnetic signal at a lift height of 10 nm, showing that whatever frequency variation that is detected comes from the magnetic stray field of the caps. Prior to the MFM measurements, a magnetic field was applied perpendicular to the Si substrate.

Figure 8 shows the magnetic contrast for magnetic caps on the spheres with a diameter of 1 000 nm. The main feature observed is a dark disk on the center of the cap and a dark ring at the sphere equator. This indicates a nonhomogeneous magnetization profile at the equator and also at the top of the cap. The same profile was observed in 500 nm spheres but now with a magnetization reversal from the equator to the top of the cap (see inset of Fig. 9). The opposite magnetization at the equator and at the top of the cap yields a black

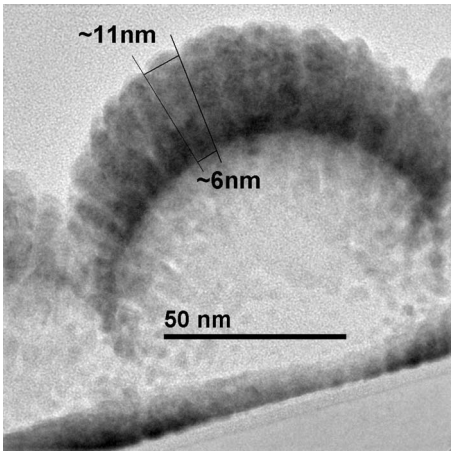

FIG. 7. TEM cross-section image of a single sphere with a diameter of 100 nm.

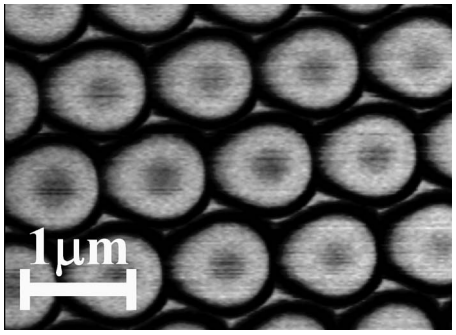

FIG. 8. Magnetic contrast obtained by MFM for 1 000 nm diameter magnetic caps.

and/or white contrast in these two regions. Despite the multilayer relative thickness, which favors an in-plane magnetization, the observed MFM contrast suggests that the magnetization at the top and at the equator are oriented perpendicular to the Si substrate plane. As for the rest of the cap, the magnetization continuously varies and no magnetic signal is detected, and since MFM images are sensitive to variations in the perpendicular component of the stray field,[23] this suggests that the magnetization in these regions lies in plane. Figure 9 shows the topographic profile combined with the magnetic signal (in hertz). It is possible to notice that the magnetic ring at the sphere equator does not completely coincide with the topographic equator. The top core, however, coincides with the center of the spheres and has a diameter of ~180 nm. This is not necessarily the size of the vortex core since MFM images are not a precise measurement of the magnetic nanostructure size. One can only say that the vortex is of the order of 180 nm.

D. Magnetization measurements

We have measured the magnetization of the caps with a superconducting quantum interference device magnetometer

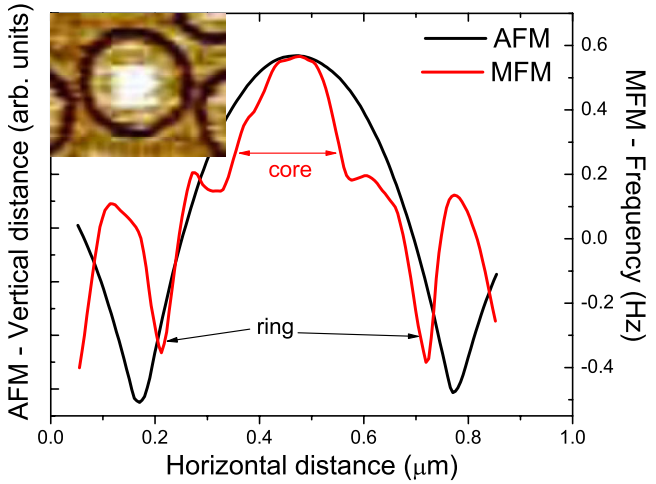

FIG. 9. (Color online) Vertical profile of the AFM (black line) and MFM [red (gray) line] signal for the 500 nm diameter cap crossing the center of the particle, and its corresponding MFM image (inset).

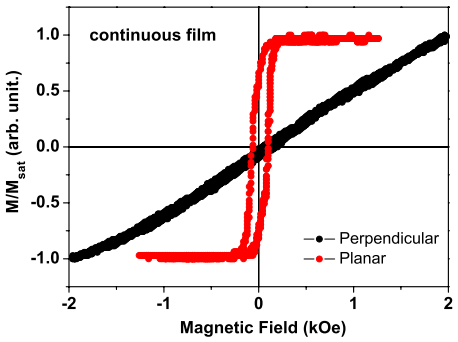

FIG. 10. (Color online) Magnetization measurement for a plane film. The black and red (gray) lines are the perpendicular and in-plane components.

and by magneto-optical Kerr effect. We show only the magnetization measurements since both exhibit the same behavior. Figure 10 shows the hysteresis cycle for the Co/Pd film deposited on Si. The measurements of the in-plane (black line) and the perpendicular (red line) magnetic components show that the magnetic anisotropy is in-plane oriented. This scenario dramatically changes for the caps. Figures 11(a)–11(d) show the magnetic hysteresis for the arrays of caps with diameters of 1000, 500, 100, and 50 nm, respectively. It is interesting to remark that for the caps, the magnetization exhibits both in-plane and out-of-plane components. The latter is more pronounced as the sphere size decreases, as can be verified by the coercivity increase in the perpendicular measurements. The presence of the in-plane and out-of-plane magnetic components is closely related to the cap shape mainly due to the film thickness gradient and curvature.

III. NUMERICAL SIMULATION

In order to interpret the MFM images and further investigate the magnetic domain formation for larger spheres (500 and 1000 nm), numerical simulations were performed. We have used a modified Heisenberg Hamiltonian given by

$$H = -\sum_{\langle i,j \rangle} J\vec{S}_i \cdot \vec{S}_j - \mu \sum_i \vec{S}_i \cdot \vec{D}_i - \mu \sum_i \vec{S}_i \cdot \vec{H}. \qquad (1)$$

The first term corresponds to the ferromagnetic exchange coupling (J is the exchange constant), the second term is associated with the dipolar interaction, and the last one is the Zeeman energy (μ is the magnetic moment per cell and $\vec{S}_i$ is the normalized moment). $\vec{D}_i$ and $\vec{H}$ are the dipolar and applied magnetic fields, respectively, being $\vec{D}_i = \mu(\Sigma_j \frac{-\vec{S}_j}{r_{ij}^3} + 3\vec{r}_{ij}\frac{\vec{S}_j \cdot \vec{r}_{ij}}{r_{ij}^5})$. We have taken into account the cap thickness variation following a cosine dependence, as experimentally observed in the TEM analysis. The lower energy configuration was obtained, minimizing the total energy through gradient like methods.[24] Similar results were obtained using the Monte Carlo method, as well. We have used the $J = 1 \times 10^{-6}$ erg/cm, $M_s = 700$ emu/cm^3, and the cell size equal to 5 nm. The simulations follow the experimental protocol; it

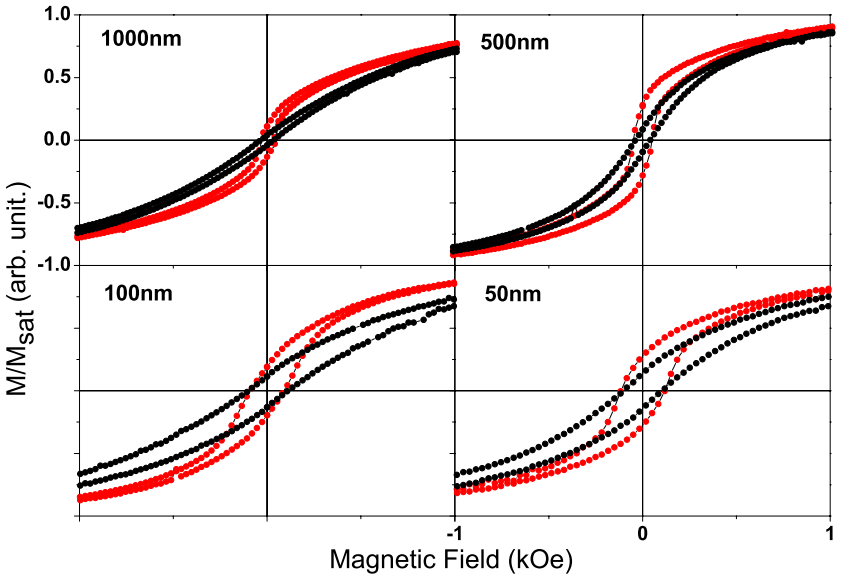

FIG. 11. (Color online) Magnetization measurements for 1000, 500, 100, and 50 nm. The black and red (gray) lines are the perpendicular and in-plane components.

was performed at the remanence after a field applied perpendicular to the plane defined by the spheres.

Figure 12 shows, from the top view, the magnetic domain structure obtained for the cap with a diameter of 500 nm. At the edge, one sees the moments pointing up and oriented parallel to the surface and, close to the top, the moments are in-plane oriented, curling around the center with a small and increasing perpendicular magnetic component pointing inward. In order to go further in the model and to compare to the experiments, we have calculated the corresponding MFM contrast of the moment configuration shown in the Fig. 12. The MFM signal was calculated from the second derivative of the stray field in relation to the distance of the cap surface $\partial^2 B/\partial z^2$ (see inset of Fig. 12). The agreement between the experimental MFM image and the one from simulations is clear.

It is interesting to remark that no anisotropy term was included in the Hamiltonian. The good agreement between the experimental and the simulation results means that only the shape anisotropy, which comes from the dipolar interaction integrated over the overall cap volume, is responsible for the observed magnetic configuration. The exchange interaction plays an important role, as well, since it determines the vortex size. The smaller the exchange coupling is, the larger is the vortex on the caps.

In order to further understand the magnetic domain structure, we have simulated the domain pattern under a magnetic field and explored the dynamics on the magnetization reversal. We calculated the hysteresis cycle with the magnetic field applied perpendicular to the plane of the spheres. To illustrate the magnetic dynamics, the cap was divided in horizontal rings (see inset of Fig. 13) and we calculated the coercive field (H_C) for each ring. As can be seen in Fig. 13, it is the intermediate region between the top and the edge that first reverse the magnetization, followed by the edge, and then by the top. The intermediate region corresponds to the base of the vortex that is magnetized almost parallel to the plane of the spheres. Thus, the rings in the intermediate region rotate their magnetization and the base of the vortex moves down to the edge, inducing its magnetization reversal

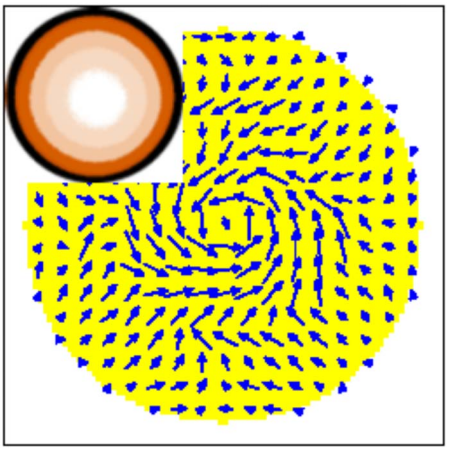

FIG. 12. (Color online) Magnetic domain configuration of a single sphere with a diameter of 500 nm and the corresponding MFM contrast (inset) obtained by simulation.

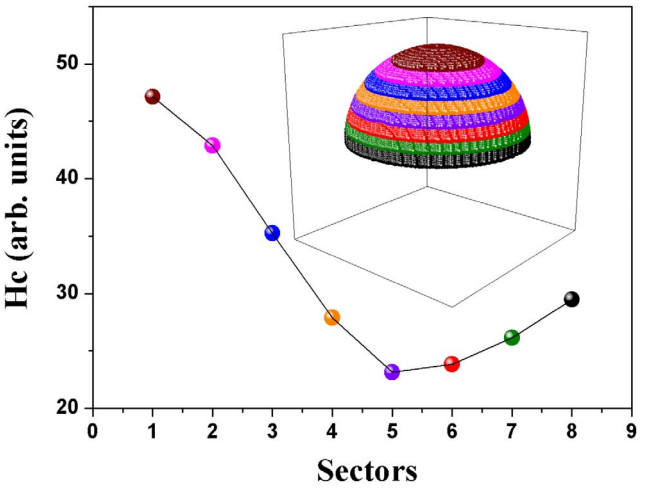

FIG. 13. (Color online) Coercive field for different slabs of the 500 nm cap obtained from the micromagnetic simulations.

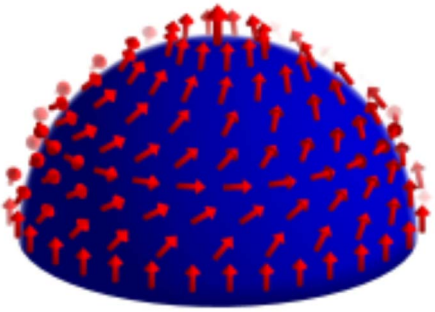

FIG. 14. (Color online) Sketch of the magnetic moment configuration for large spheres (500 and 1000 nm).

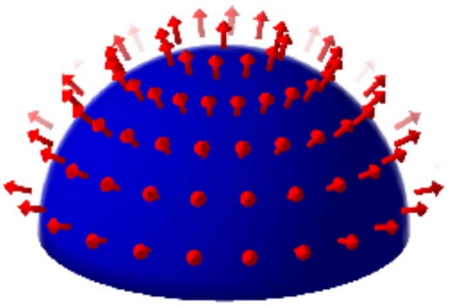

FIG. 15. (Color online) Sketch of the magnetic moment configuration for small spheres (50 and 100 nm).

for a field a bit larger. The same process occurs for rings above the intermediate region; the magnetization of the rings rotates and attains their $H_C's$ for larger field values, finishing at the top of the cap with the largest H_C.

The same simulations performed for smaller sizes produce similar behavior. Compared to the dependence found for the 500 nm cap, the only difference is that the smaller caps do not exhibit a minimum value. The coercivity on the top has the same value as the 500 nm cap, and decreases and saturates for other rings. However, we have to be careful with this analysis because real caps cannot be continuous films, as it happens for small caps (50 and 100 nm), and therefore, such approach on the simulations are no longer valid.

IV. DISCUSSION AND CONCLUSIONS

On the light of the simulations, the observed contrast on the MFM images at the edge of the caps, i.e., the ring, indicates that there exist a magnetic component tangential to the sphere surface (perpendicular to the plane of the spheres). It is worth noticing that due to the variable thickness, a change in the anisotropy direction should be expected at some point between the top and the edge. Thus, at the edge, the surface anisotropy would provide a magnetization perpendicular to the cap surface. However, as seen above, the TEM analysis at the edge have shown a granular structure and rough Co/Pd interfaces. As a consequence, the surface anisotropy vanishes and the shape anisotropy is favored, providing the in-plane magnetic orientation.[9] Since the MFM measurements are performed at the remanence, i.e., after the application of the saturation field, the magnetization at the edge remains aligned along the same direction, forming the ring. Above the ring, as seen in Figs. 8 and 9, in MFM measurements and according to the simulations, the intermediate and intense MFM contrasts correspond to a magnetization curling with a core on the top pointing up or down.

The observed core size is much larger than the ones observed in the planar disks, which is around 10 nm.[10,12] As it is well known in planar disks, the angle between the adjacent moments becomes large when close to the center and, to decrease the exchange interaction, the moments turn out of plane, being normal to the disk. For spheres with diameters of 500 and 1000 nm, the size of the vortex core is approximately 180 and 300 nm, respectively. Such enlargement is due to the sphere curvature. Another point to be discussed is related to the dipolar interaction among the caps. We did not find any characteristic pattern corresponding to the interaction among the caps as nearest-neighbors ring or core magnetic moments point up and down such as a checkerboard like structure.[20,21,25,26]

A picture of the resulting magnetic domain for larger caps (500 and 1000 nm) is depicted in Fig. 14. There exists a vortex with a core on the top due to the increasing magnetic component going to the top and, at the edge, the moments are pointing perpendicular to the plane defined by the spheres. On the other hand, for smaller sphere sizes (50 and 100 nm), considering each nanopillar in which the cap is segmented as an individual particle, the shape anisotropy favors in the magnetization to be oriented along the column axis, leading to an effective radial magnetic anisotropy. Figure 15 shows a sketch of what should be the magnetic moment configuration for the spheres with sizes of 50 and 100 nm. However, further investigation using techniques capable of probing the magnetization with nanoscale resolution such as the spin polarized scanning tunneling microscopy, for instance, is needed.

In summary, we have studied the magnetic domain formation in three-dimensional nanostructures and nanomagnetic caps using high resolution transmission electron and scanning probe microscopies. These results can have some importance to magnetic-recording media since they indicate that it is possible to tailor the effective anisotropy of the magnetic nanospheres by properly combining the sphere size with the intrinsic thin film magnetic anisotropy. In particular, it is possible to obtain a very well defined effective perpendicular magnetic anisotropy using thin films with an intrinsic planar anisotropy just by changing the substrate shape, i.e., by varying the sphere diameter.

ACKNOWLEDGMENTS

We thank the Brazilian agencies CNP$_q$, CAPES, FAPERJ, and FAPESP for financial support, as well as the microscopy facilities (LME, LMT, LMF) of the LNLS for the technical support on microscopy techniques.

*sampaio@cbpf.br

[1] J. I. Martin, J. Nogues, K. Liu, J. L. Vicent, and I. K. Schuller, J. Magn. Magn. Mater. **256**, 449 (2003).
[2] S. D. Bader, Rev. Mod. Phys. **78**, 1 (2006).
[3] S. Honda, Y. Ikegawa, and T. Kuasada, J. Magn. Magn. Mater. **111**, 273 (1992).
[4] W. R. Bennett, C. D. England, D. C. Person, and C. M. Falco, J. Appl. Phys. **69**, 4384 (1991).
[5] U. Gradmann, Appl. Phys. **3**, 161 (1974).
[6] J. I. Hong, S. Sankar, A. E. Berkowitz, and W. F. Egelhoff, Jr., J. Magn. Magn. Mater. **285**, 359 (2005).
[7] S. Landis, B. Rodmacq, B. Dieny, B. DalZotto, S. Tedesco, and M. Heitzmann, Appl. Phys. Lett. **75**, 2473 (1999).
[8] X. Zhang, M. H. Manghnani, and A. G. Every, Phys. Rev. B **62**, R2271 (2000).
[9] C. Chappert, H. Bernas, J. Ferré, V. Kottler, J. P. Jamet, Y. Chen, E. Cambril, T. Devolder, F. Rousseaux, V. Mathet, and H. Launois, Science **280**, 1919 (1998).
[10] T. Shinjo, T. Okuno, R. Hassdorf, K. Shigeto, and T. Ono, Science **289**, 930 (2000).
[11] C. L. Chien, F. Q. Zhu, and J. G. Zhu, Phys. Today **60**(6), 40 (2007).
[12] A. Wachowiak, J. Wiebe, M. Bode, O. Pietzsch, M. Morgenstern, and R. Wiesendanger, Science **298**, 577 (2002).
[13] W. Jung, F. J. Castano, and C. A. Ross, Phys. Rev. Lett. **97**, 247209 (2006).
[14] B. Van Waeyenberge, A. Puzic, H. Stoll, K. W. Chou, T. Tyliszczak, R. Hertel, M. Fhnle, H. Brckl, K. Rott, and G. Reiss, Nature (London) **444**, 461 (2006).
[15] V. Pribiag, I. Krivorotov, G. Fuchs, P. M. Braganca, O. Ozatay, J. C. Sankey, D. C. Ralph, and R. A. Buhrman, Nat. Phys. **3**, 498 (2007).
[16] K. Yamada, S. Kasai, Y. Nakatani, K. Kobayashi, H. Kohno, A. Thiaville, and T. Ono, Nat. Mater. **6**, 270 (2007).
[17] R. Cowburn, Nat. Mater. **6**, 255 (2007).
[18] N. D. Denkov, Langmuir **8**, 3183 (1992).
[19] Robert C. O'Handley, *Modern Magnetic Materials: Principles and Applications* (Wiley, New York, 1999).
[20] M. Albrecht, G. Hu, I. L. Guhr, T. C. Ulbrich, J. Boneberg, P. Leiderer, and G. Schatz, Nat. Mater. **4**, 203 (2005).
[21] T. C. Ulbrich, D. Makarov, G. Hu, I. L. Guhr, D. Suess, T. Schrefl, and M. Albrecht, Phys. Rev. Lett. **96**, 077202 (2006).
[22] J. Moritz, F. Garcia, J. C. Toussaint, B. Dieny, and J. P. Nozières, EPL **65**, 123 (2004).
[23] D. Sarid, *Scanning Force Microscopy with Applications to Electric Magnetic, and Atomic Forces* (Oxford University Press, New York, 1991).
[24] J. Miltat, G. Albuquerque, and A. Thiaville, in *Spin Dynamics in Confined Magnetic Structures I*, edited by B. Hillebrands and K. Ounadjela (Springer, New York, 2001), p. 1.
[25] L. C. Sampaio, M. P. de Albuquerque, and F. S. de Menezes, Phys. Rev. B **54**, 6465 (1996).
[26] L. C. Sampaio, R. Hyndman, F. S. de Menezes, J. P. Jamet, P. Meyer, J. Gierak, C. Chappert, V. Mathet, and J. Ferré, Phys. Rev. B **64**, 184440 (2001).